

Ab initio study for the low-lying electronic states of Al_3 and Al_3^- : The photoelectron spectroscopy of Al_3^-

Kyoung K. Baeck

Department of Chemistry, Kang-Nung University, Kang-Nung, 210-702, Korea

Rodney J. Bartlett

Quantum Theory Project, University of Florida, Gainesville, Florida 32611

(Received 24 April 1997; accepted 10 March 1998)

The low-lying electronic states of Al_3 (${}^2A_1, {}^2B_1, {}^4A_2, {}^4B_1, {}^2B_2, {}^2A_1, {}^4B_2, {}^6A_2$) and Al_3^- (${}^1A_1, {}^3B_2, {}^3A_1, {}^3A_2, {}^3B_1, {}^5A_2$) are studied by coupled-cluster methods with a $[6s5p2d1f]$ basis set. The geometries and harmonic frequencies are calculated by the coupled-cluster single double triple (CCSD(T)) correlation method with frozen core and virtual molecular orbitals. The energetic splittings at CCSD(T) geometries are calculated also by the CCSDT method. The calculated vibrational frequencies of the observed states of Al_3 (${}^2A_1, {}^2B_1$, and 4A_2) and Al_3^- (1A_1 and 3B_2) are in excellent agreement with experimental results. Other frequencies of this work are expected to be correct within $\pm 20 \text{ cm}^{-1}$. It is shown that ${}^4A_2-{}^4B_1({}^4E'')$ and ${}^2B_2-{}^2A_1({}^2E')$ of Al_3 as well as ${}^3B_2-{}^3A_1({}^3E')$ and ${}^3A_2-{}^3B_1({}^3E'')$ of Al_3^- are pairs of minima and transition states on a potential energy surface of a pseudorotation of the corresponding degenerate states. The vertical excitation energies of additional states of Al_3 (${}^2E', {}^4E', {}^2A_1'$) and Al_3^- (${}^1E'', {}^1E'$) are calculated by the electron-excitation equation-of-motion CC method and the electron-attachment equation-of-motion CC method. The possible processes of ionizations and vibronic transitions are analyzed based on the calculated results. All features of the recent photoelectron spectroscopic study of Al_3^- are explained consistently. It is also shown that the photoelectron signals of electron binding energies of 2.65 and 4.4 eV in earlier experiments correspond to the ionization of the ground state of Al_3^- to higher-lying excited states of Al_3 . The two states of the resonant two-photon ionization experiment are assigned to the lowest quartet state and the third quartet state, ${}^4E'' \rightarrow {}^4E'$, without ambiguity. The anticipated features of five more electronic excitations with transition energies of 0.22, 0.69, 0.77, 0.98, and 1.06 eV are discussed. © 1998 American Institute of Physics. [S0021-9606(98)00423-1]

I. INTRODUCTION

The availability of laser vaporization experimental techniques has stimulated many studies on small metal clusters, and the diversity of their electronic structures has been the subject of several experimental and theoretical studies. One of the simplest possible metal clusters, the aluminum trimer is a prototype, but it is not understood. The trimer has several low-lying, closely spaced electronic states, and their exact characterization offers a challenge to both sophisticated experiments and high-level theoretical calculations. With the aid of the latter, we will attempt to offer a consistent identification of all the current experimental data, and a prediction of, as yet, unobserved features.¹⁻³

Even the identity of the ground state of Al_3 has been controversial. The first experimental result by electron spin resonance (ESR) in hydrocarbon matrices⁴ suggested the 4A_2 state (in D_{3h}) to be the lowest, while a Stern-Gerlach measurement in a supersonic beam⁵ with helium and neon carrier gas reported a doublet ground state. The results of theoretical studies in that period added to the controversy. Some calculations supported ${}^2A_1'$ (Refs. 6 and 7) while others found the 4A_2 state as the lowest, though they did not specify a ground state;⁸ and even 4B_1 (Ref. 9) as the lowest state. A later calculation¹⁰ showed that ${}^2A_1'$ and 4A_2 states are virtually

degenerate, and that the 4B_1 state is the transition state while the 4A_2 is the minimum state on the potential energy surface of pseudorotation of the degenerate ${}^4E''$ state. A later ESR study in a noble gas matrix with better temperature control¹¹ convincingly argued that the ${}^2A_1'$ state is the ground state.

The search for other low-lying electronic states of Al_3 was conducted mainly by photoelectron spectroscopy of jet-cooled Al_3^- . One¹² or two¹³ electronic states of Al_3 corresponding to electron detachment processes from Al_3^- are observed in earlier works with 6.42 and 3.68 eV photon energies, respectively, but no information except electron binding energies are provided because of low resolution. The later photoelectron spectra of Al_3^- with 5.0 and 3.68 eV UV light observed five peaks (A, B, C, X, and Y), but no information about their vibrational properties.² The authors assigned three of them (A, B, and C) to electron detachment processes from the ground state of the anion to excited states of neutral aluminum trimers, while the other two (X and Y) were assigned to impurities or excited anions with uncertainties. Resonant two-photon ionization³ observed some state. Though the study provided the vibrational properties of the state, the identity of the state was not determined. Another observation of the vibronic transition between the low-lying electronic states of Al_3 was also recently reported.¹⁴

In spite of all these efforts, parts of these experimental

results are not yet understood, and there are discrepancies between the previous theoretical results on the properties of the low-lying states, such as the geometries, vibrational properties, as well as the order and energetic splittings between them.

In a recent unpublished work, Villalta and Leopold measure the photoelectron spectrum of Al_3^- to high resolution ($\pm 20 \text{ cm}^{-1}$), and thereby obtain reliable information on vibrational properties and energetic properties.¹ Though their analysis is consistent and reliable, the vast diversity of states for the Al_3 system and their geometrical parameters are not revealed, partly because their experiments are limited to electron binding energies less than 2.540 eV, and partly because their analyses are based upon observed signals with only limited results from theoretical studies. As yet, no theoretical results have been able to explain the many observations in a consistent manner.

In order to understand the features, it is requisite to have reliable theoretical results for energetic properties and for vibrational properties. The purpose of this work is to provide such information by high level *ab initio* correlated methods, and to discuss the relationships among the low-lying states of the neutral and negatively charged aluminum trimer.

According to previous theoretical studies and some available experimental results, the adiabatic energetic splittings between these low-lying states are only a few tenths of an electron volt. The harmonic frequencies range from 150 to 350 cm^{-1} , and their differences are just a few tens of cm^{-1} . In order for theoretical results to be informative enough for these states, a proper treatment of electron correlation is indispensable. We use highly accurate coupled-cluster (CC) methods to study the geometries, electronic energies, and harmonic frequencies of the electronic states of Al_3 ($^2A_1, ^2B_1, ^4A_2, ^4B_1, ^2B_2, ^2A_1, ^4B_2, ^6A_2$) as well as of Al_3^- ($^1A_1, ^3B_2, ^3A_1, ^3A_2, ^3B_1, ^5A_2$). In addition to these states, the excitation energies of other states are calculated with the electron-excitation equation-of-motion CC method (EE-EOM-CCSD),¹⁵ and the electron-attachment equation-of-motion CC method (EA-EOM-CCSD),¹⁶ at the geometry of the $X \ ^2A_1'$ state of Al_3 .

The details of the computational methods are described in Sec. II, followed by the main results. All possible transitions corresponding to electron detachment processes between these states are considered. The observed spectra are analyzed, and unobserved or unassigned spectra can be anticipated and reassigned based upon the calculated results.

II. COMPUTATIONAL DETAILS

In contrast to Al_2 systems, where several extensive studies with bases containing *f* functions are reported,^{17,18} no comparable theoretical study is yet available for the Al_3 systems. The extensive theoretical studies on low-lying states of Al_2 showed the necessity of the inclusion of *f* functions in the basis plus high-level correlation in obtaining the closely spaced states, while the effects of core correlation were negligible.

We believe that the main reason for discrepancies between the results of previous theoretical studies on Al_3 stem

from an inadequate size of bases. The results of a preliminary study¹⁹ on Al_3 by the coupled-cluster single and doubles (CCSD),²⁰ and inclusion of noniterative triples [CCSD(T)]²¹ methods with PVDZ ($12s8p1d$)/[$4s3p1d$], TZ2P ($12s9p2d$)/[$6s5p2d$], PVTZ ($15s9p2d1f$)/[$5s4p2d1f$], and TZ2PH ($12s9p2d1f$)/[$6s5p2d1f$] basis sets also showed that the inclusion of an *f* function (and triple excitations in correlations) make changes of -0.01 (-0.01) Å on bond length, $+300$ ($+500$) cm^{-1} on the $^2A_1 \rightarrow ^2B_1$ adiabatic transition energy, and $+10$ ($+10$) cm^{-1} on the symmetric stretching frequency, respectively, while the effects of frozen core electrons ($1s, 2s, 2p$ electrons) are about $+0.01$ Å, -100 cm^{-1} , and $\pm 2 \text{ cm}^{-1}$, respectively. 95% of the computation time can be saved by the frozen core approximation without hurting the results. Based on these results, the CCSD(T) method with a basis set including an *f* function are used while core-correlation effects are neglected in all calculations.

A basis of triple-zeta double polarization and the next *higher* polarization function, TZ2PH ($12s9p2d1f$)/[$6s5p2d1f$], is constructed from the McLean–Chandler ($12s9p$)/[$6s5p$] basis set²² by arguing two *d* functions ($\zeta=0.100, 0.315$) and one *f* function ($\zeta=0.240$). Spherical polarization functions ($5d, 7f$) are used. Because of possible unrestricted Hartree–Fock (UHF) spin contamination among the closely spaced multiplet states, restricted open-shell Hartree–Fock (ROHF) reference functions²³ are used for all open-shell cases throughout this work. This makes the reference functions less ambiguous for single reference CC methods, but as discussed elsewhere, correlated results should be close²⁴ and will have similar residual spin contamination.²⁵ The CCSD(T) method²¹ is used for electron correlation while the thirty core electrons and three highest virtual molecular orbitals are frozen during the correlation calculations. The bond length, bond angles, and harmonic frequencies are calculated by analytic gradient methods for CC/MBPT methods with frozen molecular orbitals (MOs),²⁶ recently implemented into the ACES II program system.²⁷ The geometries are optimized starting from the C_{2v} symmetry, but constrained within D_{3h} symmetry when the bond angle becomes $60^\circ \pm 0.5^\circ$.

In order to recover the possible multireference effects on energetic properties, which might be important for reliable results on states of higher multiplicity, the total energy of each state is also calculated at the CCSD(T) geometry by the CCSDT correlation method,²⁸ using the open-shell implementation of Watts and Bartlett in ACES II, which includes all the effects of triple excitations, subject to frozen core electrons.

To make a further assessment of the quality of our methodology, the CCSD(T) method with the TZ2PH basis subject to frozen core and virtual MOs, which we believe offers the proper combination to make accurate and sufficiently informative results for low-lying states of the aluminum trimer and its anions, some selected properties of aluminum dimer and its anion are calculated. When possible, the results are compared with previous results with more extended bases, which show good agreement with experimental results.

The computed bond length and harmonic frequencies of

TABLE I. The bond lengths, bond angles, adiabatic transition energies, and harmonic frequencies of the low-lying electronic states of Al_3 by the CCSD(T) and CCSDT calculations with TZ2PH(12s9p2d1f)/[6s5p2d1f] basis.

	State symmetry	2A_1	2B_1	4A_2	4B_1	2B_2	2A_1	4B_2	6A_2
		D_{3h}	D_{3h}	C_{2v}	C_{2v}	C_{2v}	C_{2v}	D_{3h}	C_{2v}
Valence configuration ^a	α spin	3110	3110	3210	4110	2210	3110	4200	4210
	β spin	2110	3100	2100	2100	2110	2110	2100	1100
R_e (Å)		2.541	2.632	2.599	2.752	2.543	(2.68) ^g	2.906	2.559
θ (°)		60.00	60.00	69.16	55.85	64.78	(56) ^g	60.00	70.72
T_e (eV)	CCSD(T)	0.000 ^f	0.218	0.238	0.280	0.702	(0.73) ^h	1.000	2.316
	CCSDT ^b	0.000 ^f	0.190	0.214	0.256	0.688		0.975	2.402
	expt. ^c	0.000	0.192	0.298		0.708			
ω (cm ⁻¹)	(sym) ^d	360	318	320	334	349	(360) ^g	244	370
	expt. ^c	360	315	305					
	(ben) ^e	236	189	153	255	210	(300) ^g	196	194
	expt. ^c	235	195	135					

^aThe valence electronic configuration of each state is given in order $a_1b_2b_1a_2$.

^bCCSDT results at the CCSD(T) geometry.

^cObtained by photoelectron spectroscopy (Ref. 1).

^dThe symmetric stretching a_1 mode.

^eThe asymmetric stretching e' mode of D_{3h} structure and the bending mode of C_{2v} structure.

^f $E_{\text{CCSD(T)}} = -725.911\,090$ a.u.; $E_{\text{CCSDT}} = -725.912\,151$ a.u.

^gEstimated values, see discussions in the text.

^hEstimated by using the EOM-CCSD calculation.

Al_2 , $X\,{}^3\Pi_u$ (2.725 Å/283 cm⁻¹) and $A\,{}^3\Sigma_g^-$ (2.493 Å/347 cm⁻¹) are comparable to the results of the most extensive study¹⁷ by the complete-active-space self-consistent field/second-order configuration interaction (CASSCF/SOCI) method with (20s13p6d4f)/[6s5p3d2f] basis, 2.727 Å/278 cm⁻¹ and 2.492 Å/345 cm⁻¹, respectively. The dissociation energy and the adiabatic separation between the two states are calculated as the difference of the CCSDT energy at the CCSD(T) geometry, and the results (1.36 eV and 298 cm⁻¹, respectively) are also comparable to the previous results (1.40 eV and 165 cm⁻¹, respectively).¹⁷ The ground state of Al_2^- is found to be the ${}^4\Sigma_g^-$ state, and the comparison between the present

results and the previous results¹⁸ by the CCD+ST(CCD) method with [7s6p3d1f] basis for bond length, harmonic frequency, vertical and adiabatic electron affinities are, respectively, 2.570 Å/334 cm⁻¹/1.37 eV/1.43 eV vs 2.558 Å/335 cm⁻¹/1.44 eV/1.50 eV. The electron affinities of Al_2 are underestimated by about 0.07 eV by the present method, partially because the TZ2PH basis is selected for neutral rather than anionic species. This fact will be considered, as discussed later, in adjusting the electronic binding energies of Al_3^- by the present work. All other properties by the present method, however, can be considered sufficiently reliable.

Based on these brief comparisons, we expect the results

TABLE II. The bond lengths, bond angles, adiabatic transition energies, and harmonic frequencies of the low-lying electronic states of Al_3^- by the CCSD(T) and CCSDT calculations with TZ2PH(12s9p2d1f)/[6s5p2d1f] basis.

	State symmetry	1A_1	3B_2	3A_1	3A_2	3B_1	5A_2
		D_{3h}	C_{2v}	C_{2v}	C_{2v}	C_{2v}	D_{3h}
Valence configuration ^a	α spin	3110	3210	4110	3210	4110	4210
	β spin	3110	2110	2110	3100	3100	2100
R_e (Å)		2.539	2.529	2.631	2.594	(2.73) ^g	2.717
θ (°)		60.00	65.40	57.04	69.31	(54) ^g	60
T_e (eV)	CCSD(T)	0.000 ^f	0.316	0.334	0.548	(0.56) ^h	0.568
	CCSDT ^b	0.000 ^f	0.311	0.326	0.530		0.590
	expt. ^c	0.000	0.409				
ω_e (cm ⁻¹)	(sym) ^d	370	356	364	326	(340) ^g	304
	expt. ^c	360	330				
	(asy) ^e	243	209	295	137	(230) ^g	236
	expt. ^c	250	200				

^{a-e}The same definitions as those in Table I.

^f $E_{\text{CCSD(T)}} = -725.975\,916$ a.u.; $E_{\text{CCSDT}} = -725.976\,715$ a.u.

^{g-h}The same definitions as those in Table I.

TABLE III. The vertical excitation energies of Al₃ and Al₃⁻, calculated by the EE-EOM-CCSD (Ref. 15) and the EA-EOM-CCSD (Ref. 16) methods at the geometry of the X²A₁' state of Al₃.

Reference ^a	Al ₃		Al ₃ ⁻	
	state	T _e (eV)	State	T _e (eV)
RHF-1(ROHF-1)	² A ₁ '(² A ₁)	0.00	¹ A ₁ '(¹ A ₁)	0.00
RHF-2(ROHF-1)	² A ₂ '(² B ₁)	0.29	³ E'(³ A ₁ , ³ B ₂)	0.30
ROHF-1(ROHF-2)	⁴ E''(⁴ A ₂ , ⁴ B ₁)	0.43	³ E''(³ A ₂ , ³ B ₁)	0.69
RHF-1(ROHF-1)	² E'(² A ₁ , ² B ₂)	0.85	¹ E''(¹ A ₂ , ¹ B ₁)	0.98
ROHF-2	⁴ A ₂ '(⁴ B ₂)	1.44	¹ E'(¹ A ₁ , ¹ B ₂)	1.06
RHF-2(ROHF-2)	² E'(² A ₁ , ² B ₂) ^b	1.46		
ROHF-1	⁴ E'(⁴ A ₁ , ⁴ B ₂) ^c	2.15		
RHF-2	² A ₁ '(² A ₁) ^d	2.45		

^aThe reference configuration for the EA-EOM-CCSD calculations for excited states of Al₃ are as follows; RHF-1=(2110), RHF-2(3100), ROHF-1(α:3110/β:2100), and ROHF-2(α:3200/β:2100), in the sequence (a₁, b₂, b₁, a₂). The state also can be calculated from the reference configuration in parentheses.

^bThe electronic configurations are (4100/3100) and (3200/3100).

^cThe electronic configurations are (3120/2100) and (3111/2100).

^dThe electronic configuration is (4100/3100).

for the Al₃ systems given in Tables I–III and Fig. 2 to be sufficiently accurate to be informative and predictive for the low-lying states of Al₃ systems. Throughout this work, the symmetry classes of the C_{2v} group are defined by the following decomposition of the irreducible representations between D_{3h} and C_{2v}; A₁(A₁), A₂'(B₂), A₁'(A₂), A₂'(B₁), E'(A₁+B₂), and E''(A₂+B₁).

III. RESULTS AND DISCUSSIONS

A. The qualitative features of the bonding and the manifold of low-lying states

The valence electron molecular orbital (MO) configurations of Al₃ and Al₃⁻ are shown in Fig. 1. The 1s, 2s, 2p electrons of the three Al atoms occupy 15 core MOs, 7a₁2b₂5b₁1a₂, which are not shown in Fig. 1. The possible

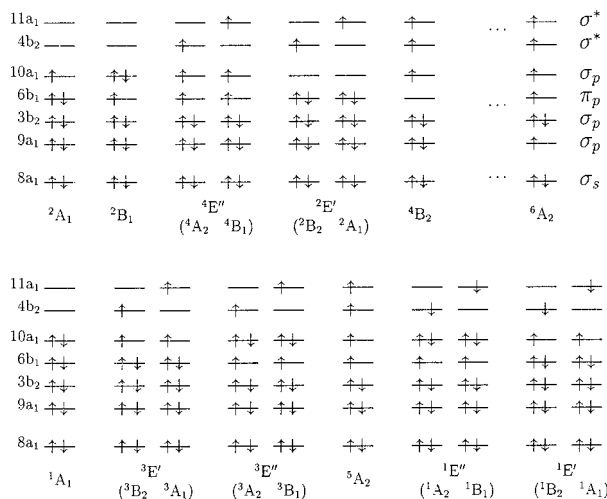


FIG. 1. The electronic MO configurations of the ²A₁, ²B₁, ⁴E'', ²E', ⁴B₂, and ⁶A₂ state of Al₃ (above) and the ¹A₁, ³E', ³E'', ⁵A₂, ¹E'', and ¹E' state of Al₃⁻ (below).

low-lying states and the splittings of E' and E'' states by the anticipated Jahn–Teller distortions are also described.

The lowest valence MO, 8a₁, can be considered as a σ_s-type bonding orbital, while the 9a₁, 3b₂, and 10a₁ MOs have σ_p-type bonding character, and the 6b₁ MO has π_p-type character. The two lowest unoccupied orbitals, 4b₂ and 11a₁, have σ* antibonding character. Because the order and the energetic separations among the 9a₁–11a₁ MOs are very small and dependent upon electronic configuration and geometrical variations, the order and the energetic separations among possible low-lying states cannot be anticipated before actual calculations with a sufficiently large basis and high-level electron correlations.

B. The geometric, energetic, and vibrational properties of the low-lying electronic states of Al₃

The ground state of the neutral trimer is the doublet state, ²A₁(²A₁') in D_{3h} symmetry, which agrees with the experiments^{1,5,11,14} and earlier theoretical results.^{6,7} The bond length is 0.02–0.08 Å shorter than previous results^{6–10} without the f function, except for the result, 2.52 Å, by density-functional methods combined with a model core potential.²⁹

The first excited state is ²B₁(²A₂') with a 0.190 eV adiabatic energy separation from the ground state, which is in good agreement with the most recent experimental value of 0.192 eV,¹ and not too far from an earlier experimental 0.219 eV¹⁴ and a theoretical result, 0.223 eV.⁶ The ²A₁→²B₁ transition corresponds to a b₁→a₁ single electron transition, roughly meaning a π→σ transition.¹⁴ The vibrational frequencies are lowered ~40 cm⁻¹ by the transition. The agreement between the calculated and experimental vibrational frequencies of ²A₁ and ²B₁ states are exceptional.

There are two quartet states, with the ⁴B₁ state falling only 0.04 eV above the ⁴A₂ state. A previous study¹⁰ showed that the ⁴B₁ state is the transition state on the potential energy surface of pseudorotation of a ⁴E'' state, while the ⁴A₂ state is the minimum on the surface. While the earlier work¹⁰ found this ⁴A₂ state to be 0.04 eV below the X²A₁ state, we find it 0.214 eV above the ²A₁ state, and this value is comparable to another theoretical result of 0.23 eV.⁶ The recent experimental value¹ for this energy separation is 0.298 eV. The energy barrier for the pseudorotation was calculated to be 676 cm⁻¹ (Ref. 6) or 2071 cm⁻¹,¹⁰ while the present result suggests that the minimum value for the barrier is 339 cm⁻¹. The vibrational frequencies we obtain (320 and 153 cm⁻¹) lie within ±20 cm⁻¹ of the experimental values (305 and 135 cm⁻¹),¹ while the earlier work produced quite different values (247, 233, and 96 cm⁻¹).¹⁰

The next excited state is either a ²B₂ or ²A₁ state which stems from the Jahn–Teller distortion of the ²E' state. Though only the geometry and vibrational properties of the ²B₂ state are calculated here, both are expected to have similar energetic and vibrational properties. Our calculation using the EA-EOM-CCSD method¹⁵ at the ²B₂ geometry locates this ²A₁ state 0.2 eV above the ²B₂ state. The energetic separation of the ²B₂ state from the ground state, 0.688 eV, by the CCSDT/CCSD(T) method compares to the recent experimental result, 0.708 eV,¹ which allows us to support assigning this state to ²B₂. A previous result for the ²B₂ state

($R_e=2.618 \text{ \AA}$, $\theta=63.2$, $T_e=0.84 \text{ eV}$)⁶ is similar. Another study⁹ produced 0.78 eV for this separation and 334 and 168 cm^{-1} for vibrations, but the wrong order of states. There are no experimental values for the vibrational frequencies of this state, but our results, 349 and 210 cm^{-1} , are expected to be good enough for further characterization of this state by experiment.

We also predict another quartet state, 4B_2 . The present result shows that this state is in D_{3h} symmetry and is non-degenerate, rather than just being a minimum of a pseudorotation of a degenerate state. The internuclear distances are noticeably longer than other states and the symmetric stretching frequency is lowered about 100 cm^{-1} , which implies electron occupation in an antibonding valence orbital. The lowest sextet state is calculated to be a 6A_2 state with a C_{2v} structure, located 2.40 eV above the ground state. Though the state falls very close to the adiabatic dissociation limit,³ the state is expected to be a bound state and will correlate to a dissociation limit with excited state fragments. The bond length is a little shorter and the symmetric stretching frequency is a little higher than the other states. There is not yet any experimental evidence supporting the existence of 4B_2 and 6A_2 states, and they cannot be easily detected by a one-electron process, as discussed later.

C. The geometric, energetic, and vibrational properties of the low-lying electronic states of Al_3^-

The ground state of Al_3^- is a singlet state with a D_{3h} structure. The computed vibrational frequencies of the ground state are in good agreement with the recent experimental result.¹ The lowest triplet states, 3B_2 and 3A_1 , fall about 0.32 eV above the ground singlet state. An earlier study⁶ found the 3A_1 state 0.40 eV above the ground state and 0.02 eV below the 3B_2 state, while the present result finds the 3A_1 state 0.02 eV above the 3B_2 state. Based on our results, one of these two triplet states can be considered to be a transition state while the other is a minimum on the potential energy surface for pseudorotation of the $^3E'$ state. A recent experiment¹ detected only the 3B_2 state. The experimental frequencies (330 and 200 cm^{-1}) agree exceptionally well with those calculated (356 and 209 cm^{-1}) in this work.

We predict an additional low-lying valence state, the 3A_2 in C_{2v} structure, located 0.53 eV above the ground state. The lowest quintet state is calculated to be the 5A_2 state in the D_{3h} structure, falling 0.59 eV above the ground state. No experimental information about 3A_2 and 5A_2 states are yet reported. The bond lengths are calculated to be a little longer and the vibrational frequencies are reduced about $30\text{--}70 \text{ cm}^{-1}$ from the other states.

There is one interesting common feature between the pseudorotations of the $^3E'$ state of Al_3^- (3B_2 and 3A_1) and the pseudorotations of the $^4E''$ state of Al_3 (4A_2 and 4B_1). When the geometries and frequencies of the two states of a pair are compared, it can be seen that the state with the shorter bond length and the wider bond angle (4A_2 of Al_3 and 3B_2 of Al_3^-) is the minimum while the other state with a longer bond length and a narrower bond angle (4B_1 of Al_3 and 3A_1 of Al_3^-) is the transition state. Though the increase in

the symmetric stretching frequency from the minimum to the transition state is marginal, the increase in the bending frequency is noticeable. Based upon this argument, the bond length, bond angle, and vibrational frequencies of the 2A_1 —the transition state of the $^2E'$ state of Al_3 in Table I—are estimated from the corresponding values of 2B_2 to be around $\sim 2.68 \text{ \AA}$, $\sim 56^\circ$, ~ 360 , and $\sim 300 \text{ cm}^{-1}$, respectively. By using the EE-EOM-CCSD method,¹⁵ the transition energy is estimated to be about 0.73 eV . By the same arguments, the properties of the 3B_1 state, which stems from the $^3E''$ state of Al_3^- are also estimated from the corresponding values of the 3A_2 , as given in Table II. Though the barrier heights and paths between the minimum and transition state of a pseudorotation are not explored here, it can be expected that two states of a pair would be connected through the asymmetric stretching mode as shown for the $^4A_2\text{--}^4B_1$ pseudorotation of Al_3 by Tse,¹⁰ and will show the fluxional behaviors shown in the ESR experiment.⁴

D. The electron detachment processes from the anion to the neutral aluminum trimer

The electronic excitation energies of neutral and negative aluminum trimers at the geometry of the X^2A_1' state of Al_3 are calculated for other states in addition to the above-mentioned states for which the geometries and vibrational properties are calculated. While the excited states of Al_3^- are calculated with the EE-EOM-CCSD methods¹⁵ with RHF and UHF references for the ground state, the vertical excitation energies of Al_3 are evaluated by the EA-EOM-CCSD method¹⁶ with two RHF and two ROHF references of Al_3^+ . The electronic configuration of the reference for the EA-EOM-CCSD calculations are (2110), (3100), (3110/2100), and (3200/2100), respectively, where the number of occupied valence orbitals are given in the sequence of (a_1, b_1, b_2, a_2) with (α/β) spins. Unlike the EE-EOM-CC, which depends upon an open-shell reference state for Al_3^- (which can complicate interpretations of excitation energies since its spin is not pure), there is no spin contamination in the EA-EOM-CC approach referenced to the Al_3^+ closed shell. However, when the same state is calculated with two different references, the difference between the two results was less than 0.12 eV . Consequently, the order of states and the energetic splittings in Table III are expected to be reliable within $\pm 0.15 \text{ eV}$.

The minimal dissociation energy of Al_3 is calculated to be 2.24 eV , but considering a possible energy barrier on the dissociation path, the upper limit on $D_0(\text{Al}_2\text{--Al})$ is suggested³ to be 2.40 eV above the lowest quartet state of Al_3 , the $^4E''(^4A_2, ^4B_1)$ state, which is 0.30 eV above the X^2A_1 state. All excited states of Al_3 in Table III are expected to be bound states.

The electron affinity (EA) of the Al atom is calculated to be 0.35 eV by the multireference double configuration interaction (MRDCI) study³⁰ and measured to be $0.441 \pm 0.010 \text{ eV}$,³¹ and the adiabatic EA of Al_2 is calculated to be 1.50 eV by the CCD+ST(CCD) study,¹⁸ and measured to be $1.6 \pm 0.1 \text{ eV}$.² Since the adiabatic EAs of Al_3 and Al_2 are 1.9 eV^2 and 1.6 eV , respectively, the dissociation energy of Al_3^- ,

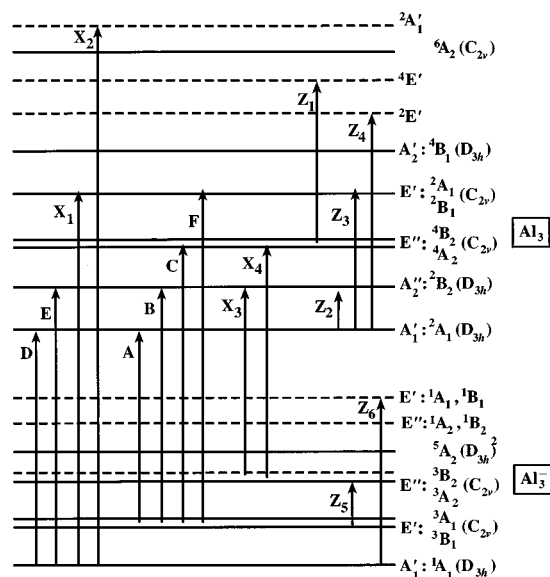


FIG. 2. The electronic states of Al_3 and Al_3^- and transitions between them. The electron detachment processes are designated by $A-F$, X_1 , and X_2 while the vibronic transitions are expressed by Z_1-Z_7 . The geometries of the states with solid horizontal lines are optimized while only the vertical excitation energies of the states with dashed horizontal lines are calculated with the EOM-CC methods. Occupation numbers of electronic states are explained in Fig. 1 and in the footnotes to Table III.

$D_0(\text{Al}_2^- - \text{Al})$ is expected to be at least 0.3 eV greater than the dissociation energy of Al_3 , $D_0(\text{Al}_2 - \text{Al})$. The minimum dissociation energy of Al_3^- , therefore, is expected to be about 2.7 eV. Moreover, because the ionization energy of Al_3^- is about 1.9 eV, all the excited states of Al_3^- in Table III are well below the dissociation limit and expected to be bound states.

All possible electron detachment processes in the aluminum trimer are shown in Fig. 2 along with the dominant electronic configuration of each state. The numbers of the occupied valence MOs are given in $(n_{a_1}n_{b_2}n_{b_1}n_{a_2}/m_{a_1}m_{b_2}m_{b_1}m_{a_2})$ notation where n_i 's stand for α spin while m_i 's for β spin, respectively. Though the meaning of the electronic configuration given in Fig. 2 becomes less clear for the higher states, the picture explains a few more facts of the observed and unobserved photoelectron spectra. We use the same designation, $A-F$, as in the experimental work¹ for the observed transitions. The additional one-electron processes are also shown with X_1 and X_2 designations, and possible electronic excitations are given as Z_1-Z_7 in Fig. 2. The results of the following discussions are summarized in Table IV.

The electron affinity corresponds to the electron binding energy of the D transition in Fig. 2. An earlier calculation reported EA of Al_3 to be 1.43 eV,⁷ which could be compared with crude experimental values at the time, 1.40 ± 0.15 eV¹³ and 1.53 eV.¹² We calculate the EA to be 1.76 eV, which is almost certainly a lower bound. According to our results, the bond lengths and vibrational frequencies of the ground states of the neutral and the anion are almost identical, and the effect of the zero-point-energy correction and the difference between vertical and adiabatic EAs are almost negligible in this case. Since the EA of Al_2 is underestimated by about

TABLE IV. The electron binding energies ($A-F, X_1, X_2$) and electron excitation energies (Z_1-Z_7) shown in Fig. 2. The electron binding energies have already been adjusted by 0.11 eV as discussed in the text. All values are in electron volts.

Transitions		Experiments		
$\text{Al}_3^- \rightarrow \text{Al}_3$	This work	PES ^a	PES ^b	
${}^3E'$ ${}^2A_1'$	A 1.60	1.51(A)		
${}^3E'$ ${}^2A_2''$	B 1.79	1.70(B)	1.7(X)	
${}^3E'$ ${}^4E''$	C 1.82	1.81(C)		
${}^1A_1'$ ${}^2A_1'$	D 1.91	1.92(D)	1.9(A)	
${}^1A_1'$ ${}^2A_2''$	E 2.10	2.11(E)	2.2(B)	
${}^3E'$ ${}^2E'$	F 2.29	2.22(F)		
${}^1A_1'$ ${}^2E'$	X_1 2.61		2.6(Y)	
${}^1A_1'$ ${}^2A_1'$	X_2 4.39		4.4(C)	

System	Transitions	This work	Experiments	
Al_3	${}^4E'' \rightarrow {}^4A_2'$	Z_1 0.77		
Al_3	${}^4E'' \rightarrow {}^4E''$	Z_2 1.85	2.03 ^c	
Al_3	${}^2A_1' \rightarrow {}^2A_2''$	Z_3 0.19	0.19, ^a 0.22 ^c	
Al_3	${}^2A_1' \rightarrow {}^2E'$	Z_4 0.69	0.71 ^a	
Al_3^-	${}^3E' \rightarrow {}^3E''$	Z_5 0.22		
Al_3^-	${}^1A_1' \rightarrow {}^1E''$	Z_6 (0.98) ^d		
Al_3^-	${}^1A_1' \rightarrow {}^1E'$	Z_7 (1.06) ^d		

^aPhotoelectron spectroscopy with 2.54 eV photon energy (Ref. 1).

^bPhotoelectron spectroscopy with 5.0 eV photon energy (Ref. 2).

^cIR spectroscopy (Ref. 14).

^dThe energy difference between corresponding vertical excitation energies.

^eThe resonant two-photon ionization (Ref. 3).

0.07 eV by the present calculations of CCSD(T) with TZ2PH basis, as mentioned in Sec. II, to assess residual errors in our calculation, we consider large basis sets. We performed calculations by the CCSD(T) method with the cc-PVQZ ($16s\ 11p\ 3d\ 2f\ 1g$)/[$6s\ 5p\ 3d\ 2f\ 1g$] basis,³² which gave 1.86 eV, consistent with the later experimental EAs of 1.90 eV (Ref. 2) and 1.92 eV.¹ Hence, to make a one-to-one correspondence between the present results and experimental results for electron binding energies of other transitions, we will include an adjustment of +0.15 eV.

The experimental results show that the intensity of D and E transitions is an order of magnitude stronger than A , B , and C transitions. Though the Boltzmann factor might help to explain the difference in the intensities of the two groups, further explanations pertain. According to our results, 1A_1 of Al_3^- has the same D_{3h} symmetry as 2A_1 and 2B_1 of Al_3 . In addition to the similar vibrational frequencies of 1A_1 of Al_3^- and 2A_1 of Al_3 , almost the same bond length (2.541 and 2.539 Å) the present calculation supports the vertical feature of the D transition with a bond angle displacement of $0.2^\circ - 0.4^\circ$ and bond length displacement of 0.005 ± 0.005 Å by the Franck-Condon fit of the experiment.¹ The bond length displacement of the E transition is calculated to be 0.093 Å, which is in good agreement with the experimental value of 0.12 ± 0.03 Å. After the correction of 0.15 eV, the calculated electron binding energies of D and E are comparable with experimental values of 1.91 and 2.10 eV (calculated) vs 1.92 and 2.11 eV (experimental).

Figure 2 shows two additional electron detachment processes, X_1 and X_2 , from the 1A_1 of Al_3^- to ${}^2E'$ (${}^2B_2, {}^2A_1$)

and 2A_1 states of Al_3 . After the correction of 0.15 eV, the electron-binding energy of the X_1 process is calculated to be about 2.61 eV, which exceeds the experimental limit of 488 nm (2.540 eV) for the photoelectron spectrum of Al_3^- .¹ The bond length and angle displacements of the transition are calculated to be rather large: 0.14 Å and 6°, respectively. Even though the Franck–Condon factor is expected not to be so large, the intensity of the X_1 transition is expected to be detectable partially because of the favorable Boltzmann factor and the one-electron nature of the process. The photoelectron spectrum with 5.0 eV photon energy,² Fig. 4 of Ref. 2, shows a peak corresponding to the electron binding energy of 2.65 eV. The authors assigned the peak, named *Y*, to impurities or excited anions. Our calculation strongly suggests that the peak corresponds to the electron detachment process from the ground anion to the third excited state, ${}^2A_1-{}^2B_2$ (${}^2E'$), of the neutral. The calculated vibrational frequencies of the 2B_2 state of Al_3 in Table I will be useful for the detection of the process in a future experiment with higher resolution.

In the same way, the electron binding energy of the X_2 process is calculated to be 4.39 eV, which can be compared with the *C* peak in the photoelectron spectrum.² The change of electron configurations implies that the process corresponds to a two-electron shake-up process, i.e., the detachment of one electron with the rearrangement of another. According to our EA-EOM-CCSD calculations,¹⁶ all other excited states fall at least 0.3 eV higher than the 2A_1 state, the final state of the X_2 process. Because this 2A_1 state is 0.2 eV above the adiabatic dissociation limit and about 0.2 eV below the upper dissociation limit observed by the resonant two-photon ionization experiment,³ it is not clear if the 2A_1 state is bound or not. The lowest possible sextet state of Al_3 is calculated to be 2.40 eV above the ground state. The lowest possible quintet state of the anion falls 0.59 eV above the ground state, and the electron binding energy for $Al_3^-({}^5A_2) \rightarrow Al_3({}^6A_2) + e^-$ is calculated to be 3.70 eV. Considering possible error bars in calculating the electron binding energy and the unfavorable Boltzmann factor, it is unlikely that the quintet state of the anion can be the source of the *C* peak.² Even though the present result cannot be definitive for the source of the *C* peak, the X_2 process in Fig. 2 is the most probable candidate for it, provided that the *C* peak actually stems from the aluminum trimer rather than any other impurity.

Four different electron detachment processes from the first excited state of Al_3^- are shown in Fig. 2 (designated as *A*, *B*, *C*, and *F* transitions), and all of them are detected by the photoelectron experiment.¹ After the estimated correction of 0.15 eV, the electron binding energies of these four peaks are calculated to be 1.60, 1.79, 1.82 and 2.29 eV, respectively, which can be compared with the experimental peaks corresponding to electron binding energies of 1.51, 1.70, 1.81 and 2.22 eV, respectively. The three processes with binding energies of 1.51–1.81 eV might be the source of the weak signal around 1.7 eV, the *X* peak in Fig. 4 of Ref. 2. The strong intensity and the vertical feature of the *F* transition can be explained from the small bond length and bond angle displacement calculated by the present work, 0.014 Å

and 0.8°, respectively, and the similar vibrational frequencies, 349 and 210 cm^{-1} (calculated) of Al_3 vs 356 and 209 cm^{-1} (calculated) or 330 and 200 cm^{-1} (experimental) of Al_3^- . The bond length and bond angle displacement of the *A* and *C* transition from the 3B_1 state of Al_3^- are calculated to be 0.01 Å/5.4° and 0.07 Å/4°, respectively, and these two transitions show similar intensities.

The experimental result also shows that the intensity of *B* is smaller than that for the *A* and *C* transitions. According to the electronic configurations in Fig. 2, the transition from ${}^3E'({}^3A_1, {}^3B_2)$ of Al_3^- to 2B_1 of Al_3 corresponds to a shake-up process, as discussed by Villalta and Leopold. The electronic configuration by our calculation confirms the shake-up nature of the *B* transition, and the change of electronic configuration can be the reason for the weaker intensity of the *B* transition.

Two transitions of electron detachment processes from the quintet state of the anion are expected to be observable. The electron-binding energies for $Al_3^-({}^5A_2) \rightarrow Al_3({}^4A_2, {}^4B_1)$ and $Al_3^-({}^5A_2) \rightarrow Al_3({}^4B_2)$ are calculated to be 1.63 and 2.30 eV, respectively. In addition to the unfavorable Boltzmann factor, the Franck–Condon factors estimated from the calculated geometries and vibrational frequencies for the two transitions are expected to be very small. Moreover, the former transition will be overlapped by the overtones of the *A* peak while the latter transition will be overridden by the *F* peak. The transition to the 6A_2 state of the neutral is expected to have very small Franck–Condon factors with the electron binding energy of 3.78 eV, which has never been observed in previous experiments.

E. The electronic excitations

The two electronic excitations observed by the resonant two-photon ionization experiment³ and the IR experiment¹⁴ are designated as Z_2 and Z_3 , respectively, and five additional possible electronic excitations are presented in Fig. 2. Considering the coupling of electronic with vibrational motion, a wider variety of transitions with weak intensities can be expected. While the features of the IR spectrum corresponding to the Z_3 in Fig. 2 are already observed experimentally¹¹ and are discussed at the beginning of Sec. III B, the Z_2 process needs some analysis here.

A high-lying electronic state of Al_3 was unexpectedly found during the spectroscopic experiment on the jet-cooled aluminum trimer.³ The transition has features of vibronic transitions from the lower-lying state with a vibrational frequency of 133 cm^{-1} , to the higher-lying state with vibrational frequencies of 205 and 273 cm^{-1} , and the lowest energy transition observed from $v=0$ is measured as 2.06 eV. Based on the observed vibrational frequencies of the ${}^4A_2({}^4E'')$ state of Al_3 ,¹ Villalta and Leopold suggest it as the transition from the 4A_2 state. Because the high-lying state has to be a quartet state, an electron detachment from a triplet state of Al_3^- can also be a possible source. However, after the correction of 0.15 eV, the electron binding energy of the process is calculated to be about 4.4 eV, and the photoelectron spectrum taken with a 5.0 eV photon (Fig. 4 of Ref. 2) shows no signal around that electron binding energy even if

we allow a ± 0.2 eV error that we believe is twice the error bar of the present calculations. This suggests that the higher-lying quartet state cannot be produced by a one-electron detachment from Al_3^- . The electronic configuration of the ${}^4E'$ state in Fig. 2, by the equation-of-motion CC method,^{15,16} also supports this interpretation. By using the above methods,^{15,16} the transition energy of the Z_2 process is calculated to be 1.85 eV. Though this value does not perfectly match the experimental³ upper limit for the ν_{00} transition, 2.06 eV, with little difficulty the excited states in Table III and Fig. 2 enable us to assign the ${}^4E'$ (${}^4A_1, {}^4B_2$) state as the high lying quartet state of the resonant two-photon ionization experiment.³

Based on the calculated electronic configurations, five more unobserved electronic transitions, Z_1 and Z_4 – Z_7 , are considered here.

The ν_{00} of Z_1 is calculated to be about 0.77 eV. Because the bond length and bond angle displacement are calculated to be ~ 0.3 Å and $\sim 9^\circ$, respectively, and because the electronic transition roughly corresponds to $\pi_p \rightarrow \sigma^*$, this transition is expected to have very weak intensity.

The ν_{00} of Z_4 is 0.69 eV by the present calculations and 0.71 eV by the photoelectron study.¹ The calculated geometries and vibrational frequencies suggest that the Franck–Condon factor of this transition is not small. This transition corresponds to $\sigma_p \rightarrow \sigma^*$, and was not yet observed by any IR experiment.

The ν_{00} of Z_5 is calculated to be 0.22 eV which is not far from the ν_{00} of Z_3 (0.19 eV, by both the present calculation and the photoelectron spectroscopic experiment¹) and, accidentally, almost the same as the observed ν_{00} in the IR experiment.¹⁴ Though the IR spectra of the experimental work is believed to stem from the neutral trimer because of several experimental conditions, the above coincidental fact is interesting. The symmetric vibrational frequency of the excited state in the IR experiment is determined to be 319 cm^{-1} , which is within the error bars of this work from the calculated frequency, 326 cm^{-1} , of the 3A_2 state of Al_3^- . Based on the calculated geometries and vibrational frequencies, the Franck–Condon factor of Z_5 is expected to be slightly smaller than that of Z_3 . The electronic transition of Z_5 also correspond to $\pi_p \rightarrow \sigma_p$, the same as of Z_3 , and the IR spectrum of Z_5 is expected to show the similar features of Z_3 .¹¹

Though the ν_{00} 's of Z_6 , and Z_7 are not calculated here because the geometries of the ${}^1E'$ and the ${}^1E''$ states of Al_3^- are not optimized, the vertical transition energies of the two transitions, 0.98 and 1.06 eV, respectively, could be helpful to future experimental work. The electronic transitions of Z_6 and Z_7 roughly correspond to $\pi_p \rightarrow \sigma^*$ and $\sigma_p \rightarrow \sigma^*$, respectively.

IV. CONCLUSIONS

Primarily based upon the cc-pVQZ results we obtained plus the earlier study of the role of diffuse functions in Al_3 and Al_3^- ,¹⁹ the estimated errors, due to basis and higher correlation corrections, of the ‘‘adjusted’’ energetic properties (electron affinity, electron binding energies, and adiabatic

energy separations) of the states calculated by the CCSD(T)/CCSDT method are thought to be about 0.1 eV for Al_3^- and slightly better for Al_3 . The bond lengths are expected to be in error by less than 0.03 Å. It appears that the calculated vibrational frequencies are accurate within $\pm 20\text{ cm}^{-1}$, which could be helpful in future experimental studies.

The results of this work show the relations between the 4A_2 and 4B_1 states of Al_3 and the 3A_1 and 3B_2 states of Al_3^- , both of which stem from one degenerate state in the Jahn–Teller distortion. The common features within the two states enable us to estimate the structure and vibrational frequencies of the transition state.

The present results show that the ground state of Al_3 is the ${}^2A_1'$ state in D_{3h} symmetry. The correct order of the low-lying electronic states seems to be established in accord with the recent photoelectron spectroscopic results.¹ In addition to offering a consistent explanation for the observed and assigned experimental signals, the present results enable assignments for the earlier experimental results and make some predictions for future observations.

It is shown that the Y peak of the photoelectron spectrum of Al_3^- with the 5.0 eV photon energy of the earlier work² corresponds to electron detachment from the ground state of Al_3^- to the third excited ${}^2E'$ (${}^2A_1, {}^2B_2$) state of Al_3 , and the seventh excited state of Al_3 , the 2A_1 , is the most probable source of the C peak² with electron binding energy of 4.4 eV. The high-lying quartet state of Al_3 , observed by the resonant two-photon ionization technique,³ is assigned to the ${}^4E'$ (${}^4A_1, {}^4B_2$) state based upon the results of the EA-EOM-CCSD method and the changes in the electronic configurations during the possible electronic excitation process. The anticipated features of the five additional electronic excitation processes (Z_1, Z_4 – Z_7 in Fig. 2) are discussed.

The analysis based on the theoretically calculated values demonstrates the relationships between the low-lying electronic states of the neutral and negative aluminum trimers. It is hoped that the unified view of this work offers a clearer understanding of their inter-relationships and aids the experimental analysis of the aluminum trimer.

ACKNOWLEDGMENTS

The authors are grateful to Professor W. Weltner, Jr., for suggesting this topic, and Professor D. G. Leopold and Professor W. Weltner, Jr. for copies of their unpublished papers and for helpful discussions. K.K.B. also appreciates generous support from Kang-Nung University. This work was supported by the U.S. Air Force Office of Scientific Research, under Grant No. AFOSR-F49620-95-1-0130.

¹P. W. Villalta and D. Leopold, Ph.D. thesis of P. W. Villalta, University of Minnesota, 1993.

²C. Y. Cha, G. Gantefor, and W. Eberhardt, *J. Chem. Phys.* **100**, 995 (1994).

³Z. Fu, G. W. Lemire, Y. M. Hamrick, S. Taylor, J. C. Shui, and M. D. Morse, *J. Chem. Phys.* **88**, 3524 (1988).

⁴J. A. Howard, R. Sutcliffe, J. S. Tse, H. Dahmane, and B. Mile, *J. Chem. Phys.* **89**, 3595 (1985).

⁵D. M. Cox, D. J. Trevor, R. L. Whetten, E. A. Rohlfing, and A. Kaldor, *J. Chem. Phys.* **84**, 4651 (1986).

⁶H. Basch, *Chem. Phys. Lett.* **136**, 289 (1987).

⁷T. H. Upton, *J. Chem. Phys.* **86**, 7054 (1987).

- ⁸L. G. M. Pettersson, C. W. Bauschlicher, Jr., and T. Halicioglu, *J. Chem. Phys.* **87**, 2205 (1987); **87**, 2198 (1987).
- ⁹G. Pacchioni, P. Fantucci, and J. Koutecky, *Chem. Phys. Lett.* **142**, 85 (1987).
- ¹⁰J. S. Tse, *J. Chem. Phys.* **92**, 2488 (1990); **96**, 1767 (1992).
- ¹¹Y. M. Hamrick, R. J. Van Zee, and W. Weltner, Jr., *J. Chem. Phys.* **96**, 1767 (1992).
- ¹²K. J. Taylor, C. L. Pettiette, M. J. Craycraft, O. Chesnovsky, and R. E. Smalley, *Chem. Phys. Lett.* **152**, 347 (1988).
- ¹³G. Gantefor, M. Gausa, K. H. Meiwes-Broer, and H. O. Lutz, *Z. Phys. D* **9**, 253 (1988); *Faraday Discuss. Chem. Soc.* **86**, 197 (1988).
- ¹⁴S. Li, R. J. Van Zee, and W. Weltner, Jr., *Chem. Phys. Lett.* **262**, 298 (1996).
- ¹⁵D. C. Comeau and R. J. Bartlett, *Chem. Phys. Lett.* **207**, 414 (1993); J. F. Stanton and R. J. Bartlett, *J. Chem. Phys.* **98**, 7029 (1993).
- ¹⁶M. Noojien and R. J. Bartlett, *J. Chem. Phys.* **102**, 3629 (1995).
- ¹⁷C. W. Bauschlicher, Jr., H. Partridge, and S. R. Langhoff, *J. Chem. Phys.* **86**, 7007 (1987); C. W. Bauschlicher, Jr., L. A. Barnes, and P. R. Taylor, *J. Phys. Chem.* **93**, 2932 (1989).
- ¹⁸K. K. Sunil and K. D. Jordan, *J. Phys. Chem.* **92**, 2774 (1988).
- ¹⁹K. K. Baeck, *Bull. Korean Chem. Soc.* **18**, 334 (1997).
- ²⁰G. D. Purvis III and R. J. Bartlett, *J. Chem. Phys.* **76**, 1910 (1982).
- ²¹J. D. Watts, J. Gauss, and R. J. Bartlett, *J. Chem. Phys.* **98**, 8718 (1993); R. J. Bartlett and J. F. Stanton, *Reviews in Computational Chemistry*, edited by K. B. Lipkowitz and D. B. Boyd (VCH, New York, 1994), Vol. 5, p. 65.
- ²²A. D. McLean, B. Liu, and G. S. Chandler, *J. Chem. Phys.* **80**, 5130 (1984).
- ²³M. Rittby and R. J. Bartlett, *J. Phys. Chem.* **92**, 3033 (1988).
- ²⁴R. J. Bartlett, in *Modern Electronic Structure Theory*, edited by D. R. Yarkony (World Scientific, Singapore, 1995), Part 1, p. 1047.
- ²⁵J. F. Stanton, *J. Chem. Phys.* **101**, 371 (1994).
- ²⁶K. K. Baeck, J. D. Watts, and R. J. Bartlett, *J. Chem. Phys.* **107**, 3853 (1997).
- ²⁷ACES II is a program product of the Quantum Theory Project, University of Florida, J. F. Stanton, J. Gauss, J. D. Watts, M. Noojien, N. Oliphant, S. A. Perera, P. G. Szalay, W. J. Lauderdale, S. R. Gwaltney, S. Beck, A. Balková, D. E. Bernholdt, K.-K. Baeck, P. Rozyczko, H. Sekino, C. Huber, and R. J. Bartlett. Integral packages included are VMOL (J. Almlöf and P. R. Taylor); VPROPS (P. Taylor) ABACUS; (T. Helgaker, H. J. Aa. Jensen, P. Jørgensen, J. Olsen, and P. R. Taylor)
- ²⁸J. Noga and R. J. Bartlett, *J. Chem. Phys.* **86**, 7041 (1987); J. Watts and R. J. Bartlett, *ibid.* **93**, 6104 (1990); *Int. J. Quantum Chem., Symp.* **27**, 51 (1993).
- ²⁹A. Martinez, A. Vela, D. R. Salahub, P. Calaminici, and N. Russo, *J. Chem. Phys.* **101**, 10677 (1994); P. Calaminici, N. Russo, and M. Toscano, *Z. Phys. D* **33**, 281 (1995).
- ³⁰U. Meier, S. D. Peyerimhoff, and F. Grein, *Z. Phys. D* **17**, 209 (1990).
- ³¹H. Hotop and W. C. Lineberger, *J. Phys. Chem. Ref. Data* **14**, 731 (1985).
- ³²D. E. Woon and T. H. Dunning, Jr., *J. Chem. Phys.* **98**, 1358 (1993).